Int. J. Adv. Sci. Eng. ***Vol.8 No.1 2025-2032 (2021)*** **2025** ***E-ISSN: 2349 5359; P-ISSN: 2454-9967***

RESEARCH ARTICLE

Numerical Simulation of Flow across a Radial Turbine for Prediction of Shaft Power for Driving Automobile Air Conditioners

G.N.Nwaji[1]*, S. Udongwo[1], K.T.Ajayi[2], D.C. Uguru-Okorie[3], E.E. Anyanwu[1]

[1]Federal University of Technology, P.M.B. 1526, Owerri, Imo State, Nigeria
[2]University of Lagos, Akoka, Yaba, Lagos, Nigeria
[3]Federal University, Oye-Ekiti, Ekiti State, Nigeria

ABSTRACT: The exhaust gas spouting from the exhaust manifold into the radial inflow turbine coupled to an exhaust pipe of a 2.5L petrol engine has been computationally simulated in order to ascertain the extent of exhaust energy recoverability for driving the vehicle auxiliaries, using Autodesk CFD. In order to determine the amount of power available at the turbine shaft at varying engine speeds, properties of the flow and fluid spouting into the turbine from the engine and out of the turbine from the volute outlet were examined by applying the $SST\ k-\omega$ turbulence model and advanced $Petrov-Galerkin's$ advection scheme. For the test engine used with the operating range of 2000-6000rpm, at engine speeds up to 3000rpm, the available power was about 0.3kW. At 4000rpm, about 2.8kW of power is available at the turbine shaft, increasing to 7.7kW at 5000rpm and 43.6kW at 6000rpm. Curve-fitting shows that at 5500rpm, as much as 15kW reversible power can be extracted from a shaft coupled to the turbocharger turbine. With an electrically-assisted turbine component of the turbocharger used, the compressor of vapour compression refrigeration system of the vehicle will be efficiently driven at all engine speeds while exhaust energy recovery is achieved.

KEYWORDS: Vaned Single-Entry, Flow Properties, Radial Inflow Turbine, Shaft Power, Turbine Reversible Power, Automobile Auxiliaries, Computational Fluid Dynamics.

https://doi.org/10.29294/IJASE.8.1.2021.2025-2032

©2021 Mahendrapublications.com, All rights reserved

INTRODUCTION

The internal combustion engine (ICE) has witnessed great progressive improvements in terms of design, configuration and in-cylinder flow optimizations towards improving the overall efficiency, fuel economy and net power developed by the engine. However, thermal efficiency still hovers around 30-50%, out of which some percentage goes into driving the parasitic auxiliaries such as the alternator, air conditioner compressor, water pump, the steering pump, etc. This invariably leads to great reduction in effective power. The energy of fuel lost through the exhaust system of an is estimated to be between 30-40%.Interests have increased tremendously in finding optimum means of harnessing this enormous waste energy [1-3]. John and Scott [4] however showed that at a speed 1500rpm and $\frac{1}{4}$ load, the exhaust heat waste was 21% and at a speed of 4500rpm and full load, the exhaust heat waste was as high as 44%.

Nowadays, emission control has become topical issues and stringent policies are applied in various countries of the world to limit emissions to certain levels. Various efforts have been made to reduce the emission of carbon (IV) oxide (CO_2) and Chlorofluorocarbons (CFCs) which are major greenhouse gases that contribute immensely to global warming and climate change. Systems like the catalytic converters, exhaust gas recirculation, engine downsizing and a host of others have been developed. In internal combustion engines (ICE), engine downsizing is an established method for the reduction of CO_2 [1, 5]. This is possible as a result of the advent of the turbochargers, which reclaim the waste fluid and kinetic energy inherent in the exhaust gas to improve on the volumetric efficiency. This makes reduction in engine size for the same power output possible and thus, the key principle behind engine downsizing.

According to [1] and, Singh and Srivastava [6], of the various techniques for harnessing engine waste heat, turbo-compounding with turbines similar to those found in car turbochargers has attained best maturity. Widely used in the automotive industry for IC engine turbo-charging purposes are radial inflow turbines [7, 8]. Acknowledging its importance therefore, many researchers have gone into the improvement of the turbocharger's turbine (which is actually

---

Corresponding Author: godswillmee@gmail.com

Received: 11.06.2021 **Accepted:** 15.07.2021 **Published on**: 02.08.2021

responsible for the extraction of fluid kinetic and thermal energy) performance seeing that its size is limited by space considerations. These turbo chargers have been modified to Electrically-Assisted Turbochargers (EAT) in order to address the inefficiencies that are experienced in turbochargers at low engine speeds [9]. The powerful electrical motor connected to the turbine shaft assist in driving the compressor during low engine speeds as a result of the production of insufficient exhaust gases and at high engine speeds, it acts as generator, converting the energy from the exhaust into electrical power which is channeled to drive electrical accessories [10]. This arrangement as has been suggested by Baines [11] operate in a milder working environment compared to a solely electrically driven compressor.

The various factors affecting the flow properties and invariably the power developed by the turbine have been investigated [2, 10]. With such powerful tools as the computational fluid dynamic (CFD) software, much insight has been gotten on the flow characteristics of the exhaust gases. Numerical analyses using ANSYS CFX code were carried out on steady and unsteady flows conditions in a turbocharger to ascertain the aerodynamic behaviours under steady and transient conditions of a twin-entry radial inflow turbine by [12]. Both the pulsatile and non-pulsatile flows in the twin entry turbine were investigated and clearer understandings on these complex flow structures were obtained from the results. [12, 13] carried out both experimental and numerical analyses on the turbine of a turbocharger in order to investigate the effect of the volute cross-sectional shape on the flow under pulsating conditions. They studied two different volute profiles considering in particular the aspect ratio of the cross sectional area of the turbine and concluded that for one of the particular volutes in question, the efficiency of the turbocharger was 1.8 points higher than the other. Srithar and Ricardo [14] experimentally studied a variable geometry mixed flow turbine and an equivalent nozzleless turbine. The variable geometry mixed flow turbine when compared to an equivalent nozzleless turbine showed higher peak efficiency and swallowing capacity at varying vane angle settings.

Ajayi and Ojakovo [15] have suggested exploitation of exhaust energy using the radial inflow turbine component of the turbocharger to drive the vapour compression refrigeration system (VCRS) of automobile air conditioners (A/Cs) thereby isolating the A/Cs from the conventional direct mechanical drive through the pulley coupled to the engine and magnetic clutch of the A/C compressor. Modern automobiles have air conditioners with capacities of 3kW and above [16]. A significant amount of engine power would be saved and a great deal of reduction in CO_2 emission would also be achieved if the A/C compressor is driven by the exhaust driven turbine. Nevertheless, matching the engine speed with turbine and AC compressor speeds at low and high engine speeds poses a great concern in retrofitting the conventional configuration to match the proposed system. Ajayi et al [17] numerically studied the flow properties at the outlet pipe of an automobile after expansion in the radial turbine component of the turbocharger and showed that kinetic energy of the exhaust gas can be harnessed for other applications without hampering the effectiveness of the vehicular system. Further investigations on the maximum efficiency operation point of the turbine coupled to the AC compressor as opposed to the original intended use as a turbocharger component need be done. Nwaji et al [20] in their work investigation of the effect of engine speed on the radial inflow turbine for automotive exhaust energy recovery have shown that from engine speeds ranging from 2000-5000 rpm, significant amount of energy is available at the shaft, which can be tapped for driving other vehicle auxiliaries through well articulated retrofitting of the current hood layout. This will save the engine power for other purposes and also reduce the amount of CO_2 that goes into the atmosphere. Therefore, this current study focuses on the flow and fluid properties of the exhaust gas as it moves from the turbine inlet to the outlet of the exhaust pipe at different engine speeds. The amount of reversible power available at the shaft coupled to the turbine is also investigated as well as the conditions favorable to such power availability.

2 Methodology

The 3D geometry comprising the volute, turbine and outlet pipe was designed with Autodesk Inventor and treated to reduce meshing errors. In order to reduce computation time, automatic mesh generation was carried out with no refinements done. This resulted in a sufficient mesh element distribution and density (a total of 123, 213 nodes and 435,224 elements) in the whole turbine stage and exhaust pipe, to capture the flow as shown in Fig. 1.

The Unsteady Reynolds Averaged Navier-Stokes (URANS) model has been adopted in the simulation of the flow across the turbine cascade in order to save computation time and cost. The URANS model deals with the conservation of mass, momentum and energy in the medium as expressed in Eqs 1-3 respectively [18].

$$\frac{\partial \rho}{\partial t} = -\frac{\partial(\rho u_j)}{\partial x_j} \tag{1}$$

$$\frac{\partial(\rho u_j)}{\partial t} = \frac{\partial}{\partial x_j}\left(\mu\left(\frac{\partial u_j}{\partial x_j}\right)\right) - \frac{\partial(\rho u_j u_j)}{\partial x_j} + \frac{\partial}{\partial x_j}\left(\mu\left(\frac{\partial u_i}{\partial x_j}\right)\right) - \frac{2}{3}\frac{\partial}{\partial x_j}\left(\mu\frac{\partial u_k}{\partial x_k}\right) + \mathrm{a_j}\rho - \frac{\partial P}{\partial x_j} \tag{2}$$

$$\frac{\partial(\rho T)}{\partial t} = \frac{\partial}{\partial x_j}\left(\frac{\lambda}{c_p}\left(\frac{\partial T}{\partial x_j}\right)\right) - \frac{\partial(\rho u_j T)}{\partial x_j} + \frac{\rho T}{c_p}\left(\frac{\partial v}{\partial T}\right)_p \frac{DP}{Dt} - \frac{\tau_{ij}}{c_p}\frac{\partial u_j}{\partial x_j} \tag{3}$$

The $k-\omega$ shear stress turbulence model was adopted to model turbulence as this limits the wall function, y^+ to one and is preferred to other two equation models in resolving turbulence [19]. The mathematical expressions of the two equation model are given as:

$$\frac{\partial(\rho k)}{\partial t} + \frac{\partial(\rho u_j k)}{\partial x_j} = P_k - \beta^*\rho\omega k + \frac{\partial}{\partial x_j}\left[(\mu + \sigma_k \mu_t)\frac{\partial k}{\partial x_j}\right] \tag{4}$$

$$\frac{\partial(\rho\omega)}{\partial t} + \frac{\partial(\rho u_j \omega)}{\partial x_j} = \frac{\gamma}{v_t}p - \beta\rho\omega^2 + \frac{\partial}{\partial x_j}\left[(\mu + \sigma_\omega \mu_t)\frac{\partial \omega}{\partial x_j}\right] + 2(1-F_1)\frac{\rho\sigma_{\omega 2}}{\omega}\frac{\partial k}{\partial x_j}\frac{\partial \omega}{\partial x_j} \tag{5}$$

The advection scheme used is based on the $Modified\ Petrov - Galerkin$ method. This method is a mathematical approach for solving and obtaining approximate solutions of partial differential equations with odd order.

The power produced by the turbine can be determined from the equation

$$P = \eta_T \dot{m} C_{pg} T_{01}\left(1 - \frac{1}{r_p^{\frac{\gamma-1}{\gamma}}}\right) \tag{6}$$

Where η_T is the turbine efficiency, $\dot{m}$ is the exhaust gas mass flow rate from the engine exhaust manifold, T_{01} is the exhaust gas stagnation temperature, r_p is the stagnation pressure ratio across the turbine and γ is the expansion index of the exhaust products.

The torque developed by the turbine is finally estimated from:

$$T = \frac{P}{\omega_r} \tag{7}$$

Where ω_r is the angular velocity of the turbine shaft, expressed as:

$$\omega_r = \frac{2\pi N}{60} \tag{8}$$

And N is the rotational speed of the shaft.

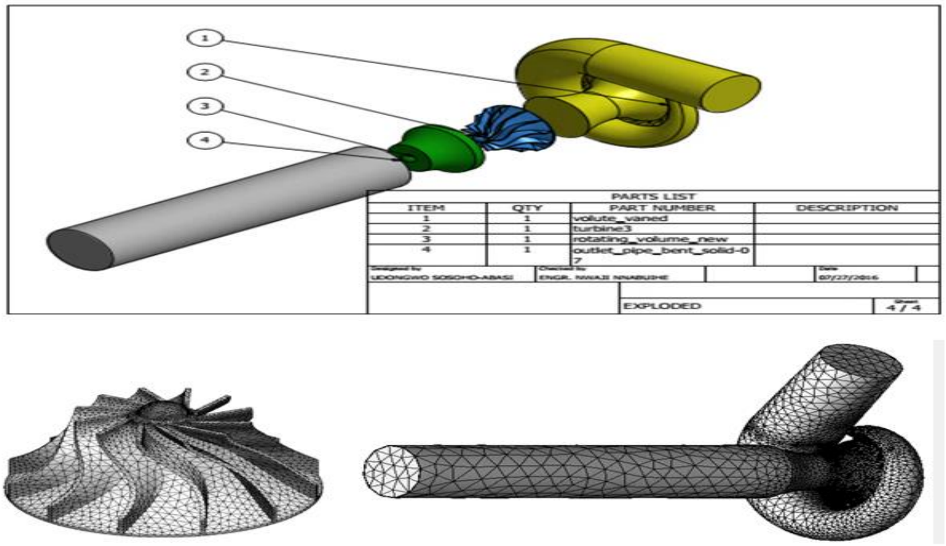

PARTS LIST			
ITEM	QTY	PART NUMBER	DESCRIPTION
1	1	volute_vaned	
2	1	turbine3	
3	1	rotating_volume_new	
4	1	outlet_pipe_bent_solid-0 7	

Designed by UDONGWO SOSOHO-ABASI
Checked by ENGR. NWAJI NNABUIHE
Date 07/27/2016
EXPLODED
Sheet 4 / 4

Fig 1: Turbine-volute-outlet pipe assembly and computational meshes

3 RESULTS AND DISCUSSION

The global axis plot line along the mid-plane of the exhaust outlet is shown in Fig. 2. The flow properties are plotted on a plane perpendicular to the flow inlet axis -the global Y axis. Values are taken along the mid axis from the tip of the turbine to the exhaust duct outlet. It covers the flow properties variation from the diverging section in the volute to the outlet pipe exit.

The variation of flow properties from the tip of the turbine to the exhaust outlet is shown in Figs 3a-g. The velocity and Mach number profiles as represented in Figs 3a and 3e take same pattern and show progressive increase from almost zero for low volume flow rates or engine speeds.Increase in velocity of the exhaust gas and the Mach Number became remarkable at engine speeds above 4000rpm. Figs 3f and 3g show that turbulent kinetic energy and turbulent energy dissipation also increase in this region. The pressure and temperature profiles are nearly linear for low engine speeds as shown in Figs 3b and 3c. For high engine speeds however, there is sharp pressure and temperature drops within the cascade region and thereafter they increased almost to initial values and remained constant throughout the outlet region. The Mach number for an engine speed of 6000rpm is supersonic. The velocity and Mach number increases till the exit of the volute diverging section. From this point, there is a decrease in velocity and Mach number, corresponding to an increase in the temperature and a reduction in static pressure. The slope of the graphs in this region, i.e. the region just after the diverging nozzle is quite erratic especially for an engine speed of 6000rpm and this may imply that there is the possibility of a shock wave developing for higher flow rates or engine speeds. Fig 3d shows that vorticity magnitude reduces along the Y-axis for all engine speeds. Temperature remains fairly constant along the length with little increases.

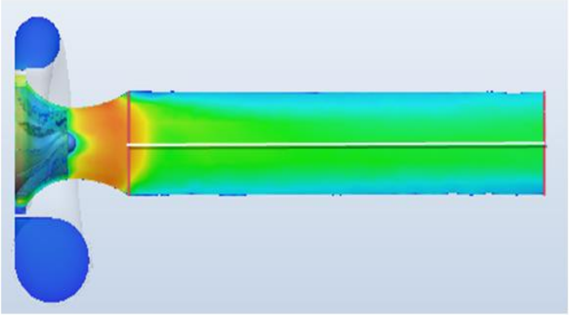

Fig. 2 Global axis plot line along the mid-plane (Y_Plot)

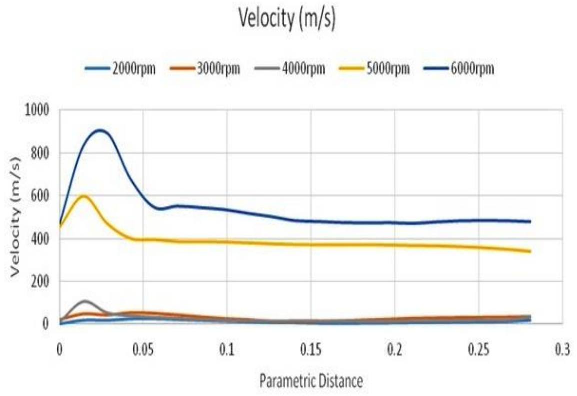

Fig.3a Variation of Velocity from turbine tip to exhaust outlet at different engine speeds

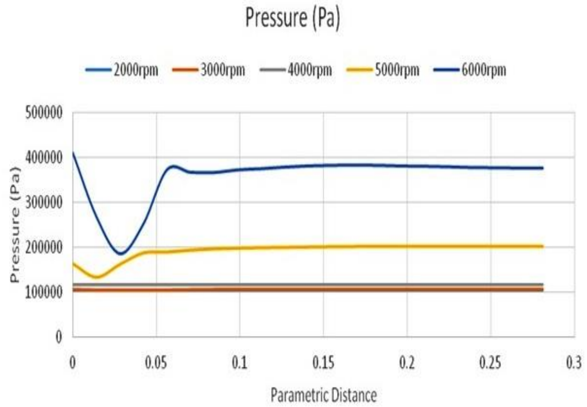

Fig.3b Variation of Pressure from turbine tip to exhaust outlet at different engine speeds

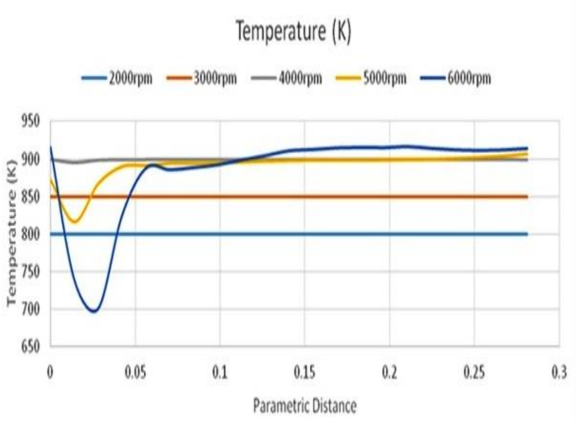

Fig.3c Variation of Temperature from turbine tip to exhaust outlet at different engine speeds

The variation of properties of the exhaust gas across the volute inlet, outlet and duct inlet at different engine speeds are shown in Figs 4-10. Fig 4 shows that at all engine speeds corresponding to low fluid flow rates, the velocity at the volute inlet experienced fairly little increases from about 20-80m/s. however, at the duct and turbine outlets, the velocity remained almost constant at low flows

Nwaji et al.,

but witnessed sharp increases at high engine speeds. The Mach number maintains the same trend with the velocity under low flows at the volute inlet and duct outlet but witnessed steep fluctuations at the turbine outlet as shown Fig. 5. From Fig. 6, the Reynolds number increases with engine speed at the inlet, duct and turbine outlets. The turbulent kinetic energy and eddy dissipation of Figs 7 and 8, respectively, are found to be constant at the volute inlet, mild variation at the duct outlet but very steep variation at the turbine outlet as the engine speed increases. From Fig. 9, while the pressure at the inlet increases at high engine speeds, it remained almost constant at the duct and volute outlets as the engine speed increases. Also, from Fig. 10, it is found that at the inlet and duct outlet, temperature increases linearly with increasing engine speed but at the volute outlet, beyond 4000 rpm, the temperature of the exhaust product starts decreasing.

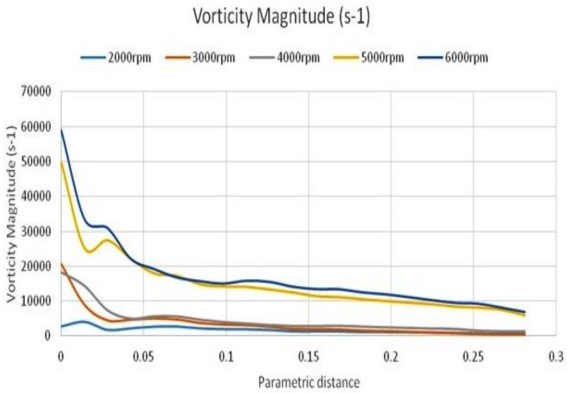

Fig.3d Variation of Vorticity from turbine tip to exhaust outlet at different engine speeds

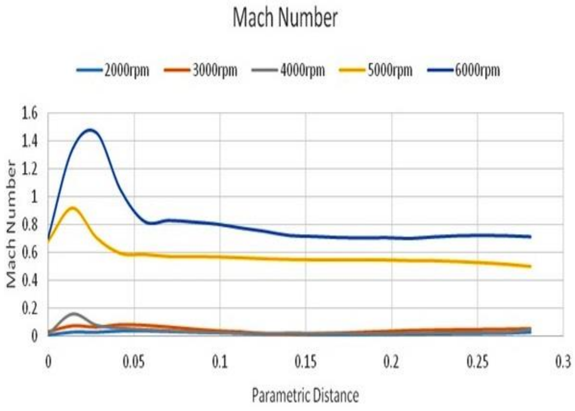

Fig.3e Variation of Mach Number from turbine tip to exhaust outlet at different engine speeds

From the inlet to the outlet, at low volume flow rates, corresponding to low engine speeds, it can be observed that there is no significant change in the temperature of the fluid. This is also observed from the very little or no change in density at such speeds. This observation is corroborated by the extremely low Mach numbers which signifies an incompressible flow if the nature and complexities of the control volume is neglected and it is considered as a control volume. At increased volume flow rates, corresponding to high engine speeds however, significant differences can be observed in the fluid and flow properties.

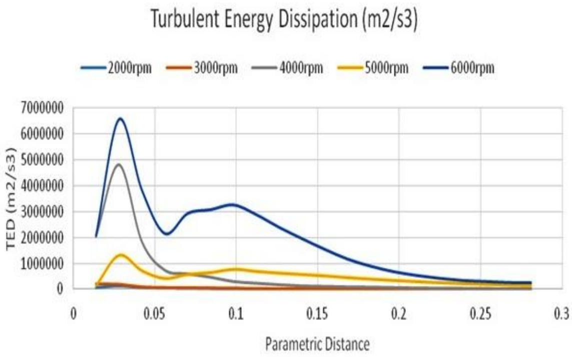

Fig.3f Variation of TED from turbine tip to exhaust outlet at different engine speeds

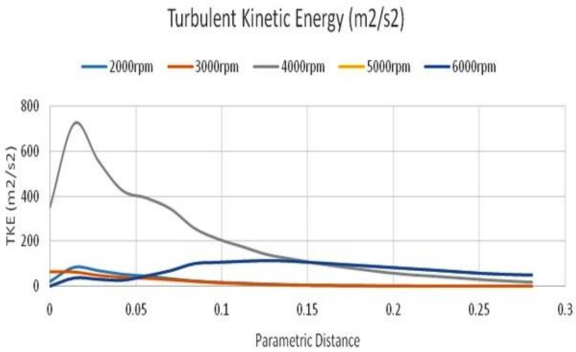

Fig.3g Variation of TKE from turbine tip to exhaust outlet at different engine speeds

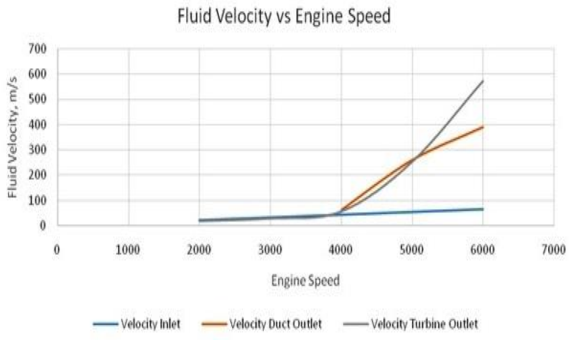

Fig. 4: Variation of fluid velocity with engine speed

The little differential pressure, ΔP that is observed, suggests that the flow is mostly kinetic energy driven. As the engine speed increases however, ΔP increases exponentially.At the turbine outlet, for low speeds, not much difference with the duct outlet values is observed except with those related to the turbulence of the flow. The turbulent kinetic energy and turbulent eddy dissipation reduce from the turbine exit to the duct outlet as the flow stabilizes. This is especially the case in relatively higher volume flow rates at increased engine speeds.

The maximum power that can be obtained at the shaft coupled to the turbine for the various loading conditions of the engine, which is given as the product of the hydraulic torque and the rotating speed of the turbine is shown in Fig. 11.

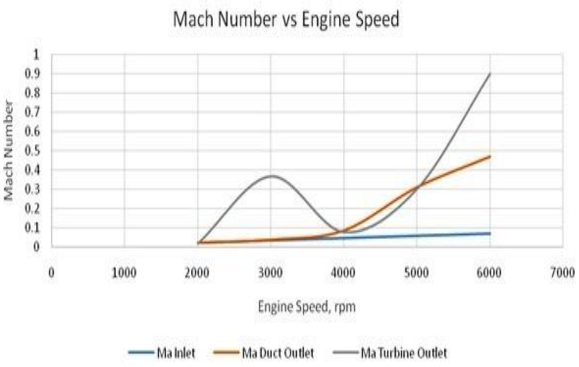

Fig. 5 Variation of Mach number with engine speed

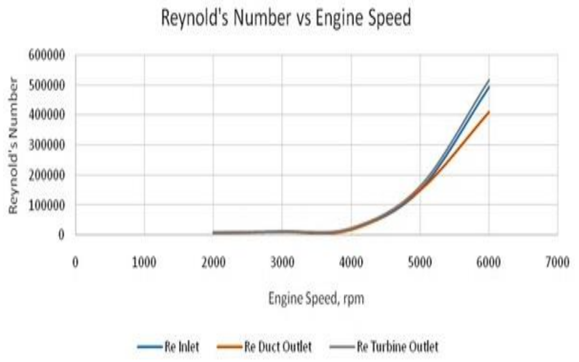

Fig. 6: Reynold's Number variation with engine speed

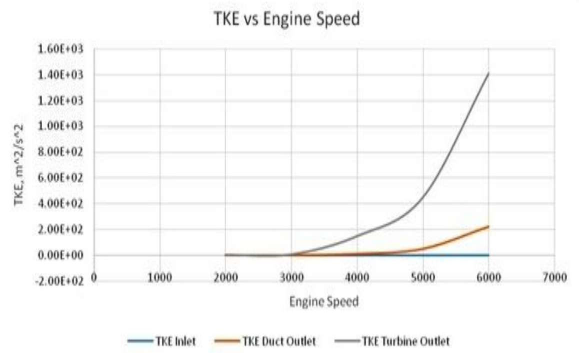

Fig 7: Turbulent kinetic energy variation with engine speed

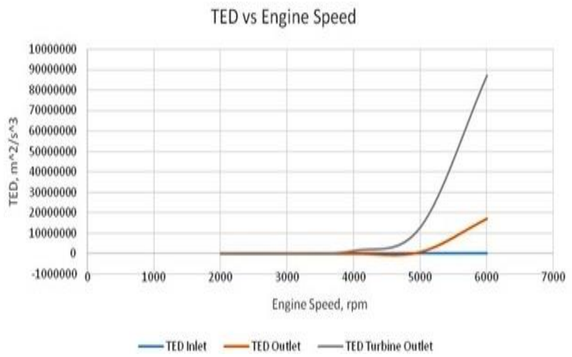

Fig. 8: Turbulent eddy dissipation variation with engine speed

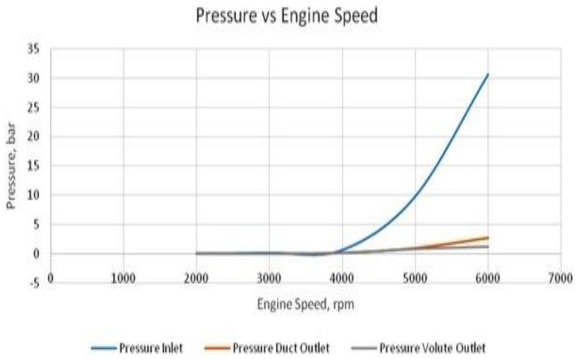

Fig. 9: Pressure variation with engine speed

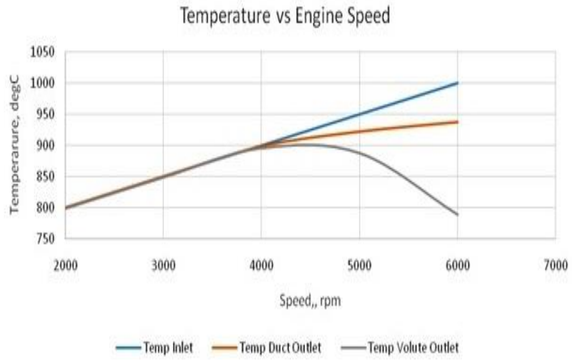

Fig. 10: Temperature Variation with Engine Speed

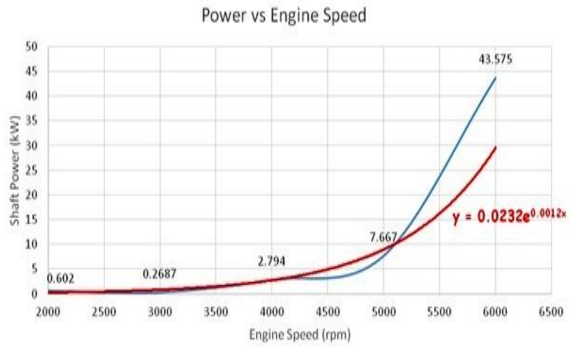

Fig. 11: Variation of shaft power with engine speed: actual plot (blue) and exponential fit (red)

From Fig. 11, it is seen that for the particular turbine size at the specified vehicle engine operation range, the power recovered at low engine speeds is very low. Significant energy recovery in terms of power is observed at engine speeds ranging from 4000-6000rpm. It is also observed that the power value at an engine speed of 6000rpm is large compared to that for other engine speeds. It is seen that as much as roughly 44kW worth of power could be obtained from the exhaust gases at such speed. However, a close look at the Y_Plot of Fig. 3e shows that at such engine speed (6000rpm), for the particular turbine size, choking occurred at the throat of the converging-diverging section of the volute geometry. This is manifested by the supersonic Mach number noticed along the Y_Plot. This may have serious effect on the scavenging capability of the engine as it results in a high back pressure (roughly 30 bars). Since the rated speed of an engine is seldom reached on normal operations, this problem is not encountered. An exponential curve fit to data points in the curve of speed against shaft power at an engine speed of 5500rpm shows that reversible power obtainable at the shaft of an exhaust gas driven single-entry vaned radial inflow turbine can get up to approximately 15kW. However, with friction and inertia effects, the effective power may be lower than the stated power. Therefore, if a smaller turbine was used for the same engine, more power would be obtained at lower engine speeds which will reduce the problem of turbo lag in the turbine and choking would occur at speeds below 6000rpm and this is a problem. In such a case, a waste-gate would be designed to reach a compromise between these two extremes.

4 CONCLUSION

Radial inflow turbines have found application in turbochargers and are used for energy extraction from exhaust gases of automobiles and a numerical investigation was done to ascertain it potential for use to drive automobile air conditioners. The simulation results obtained were based on flow properties variation across the turbine at different engine speeds and the prediction of available power at the turbine to drive the compressors of automobile air conditioners. For the test engine used, at engine speeds up to 3000rpm, the available power was about 0.3kW. At 4000rpm, 5000 rpm and 6000rpm, the available power outputs were 2.8kW, 7.7kW and 43.6kW respectively. Curve-fitting showed that at 5500rpm, as much as 15kW reversible power can be extracted from the shaft coupled to the turbocharger turbine, which is enough to drive the compressor of vapour compression refrigeration system of the vehicle. Electrically-assisted turbine component of the turbocharger is recommended for use based on the results obtained. It ensures the required torque is provided to drive the A/C compressor at low engine speeds and serve as a generator at high engine speeds. Further studies on the effect of backpressure on exhaust gas scavenging are recommended.

REFERENCES

[1] Arnaud, L.; Ludovic, G.; Mouad, D.; Hamid, Z.; Vincent, L., 2014. Comparison and Impact of Waste Heat Recovery Technologies on Passenger Car Fuel Consumption in a Normalized Driving Cycle. Energies 2014, 7: 5273-5290.

[2] Hellstroem, F., 2010. Numerical Computations of the Unsteady Flow in Turbo chargers. Royal Institute of Technology, Stocholm, Sweden.

[3] Jadhao, S.J.; Thombare, G.D., 2013. Review on Exhaust Gas Heat Recovery for I.C.E. International Journal of Engineering and Innovative Technology (IJEIT), 2 (12):

[4] John, A.R.; Scott, M.A., 2014. Review of Waste Heat Recovery Mechanisms for Internal Combustion Engines. Journal of Thermal Science and Engineering Applications.

[5] Uguru-Okorie, D.C.; Dare, A.A.; Burluka, A.A., 2016. Effect of Supercharging on Cycle-to-Cycle Variation in a Two-Stroke Spark Ignition Engine. SAE Paper 2016-01-0688.

[6] Singh, B.K.; Shrivastava, N., 2014. Exhaust Gas Heat Recovery for C.I Engines -A Review. International journal of engineering sciences & research.

[7] Ramsey, J., 2014. Why turbo compounding may be the next big thing in power trains. www.autoblog.com/2014/11/18/turbo-compounding-next-big-thing-powertrains/ (Accessed 18 November 2014).

[8] BP Group., 2016. The History of Turbo Compounding. www.bowmanpower.com/blog/the-history-of-turbo-compounding/, (Accessed 5 May 2016).

[9] Katrašnik, T.; Rodman, S.; Trenc, F., 2003. Improvement of the Dynamic Characteristic of an Automotive Engine by a Turbocharger Assisted by an Electric Motor. J. Eng. Gas Turbines Power.

[10] Mamdouh, A.; Nikolaos, X.; Apostolos, P., 2019. Modelling of Electrically-Assisted Turbocharger Compressor Performance. Energies 2019; 12: 975.

[11] Baines, N.C., 2005. Fundamentals of Turbocharging; Concepts NREC: White River Junction, VT, USA.

[12] Abidat, M.; Hachemi, M.; Hamel, M.; Hamidou, M.K., 2006. Design and Flow Analysis Of Radial and Mixed Flow Turbine Volutes. European Conference on Computational Fluid Dynamics, TU DEFT, Netherlands.

[13] Mingyang, Y.; Ricardo, M.B.; Rajoo, S.; Takao, Y.; Ibaraki, S., 2015. An investigation of volute cross-sectional shape on turbocharger turbine under pulsating conditions in internal combustion engines, Energy Conversion and Management 105: 167–177.

[14] Srithar, R.; Ricardo, M.B., 2008. Variable Geometry Mixed Flow Turbine for Turbochargers: An Experimental Study. International Journal of Fluid Machinery and Systems 1(1): 155-168.

[15] Ajayi, K.T.; Ojakovo, A.E., 2012. Design and Development of Micro-Turbine Coupled Compressor for Air-Conditioning System in Automobiles. Journal of Emerging Trends in Engineering and Applied Sciences (JETEAS) 3 (2): 259-264.

[16] Nishant, A.; Ekhlak, K., 2018. Automobile Air Conditioning System. International Research Journal of Engineering and Technology 5 (6): 2122 – 2125.

[17] Ajayi, K.T.; Nwaji, G.N.; Ojo, O.B., 2014. Numerical Study of the Properties of High Energy Gas Flow through a Micro-turbine in 3D Cascade. Journal of Emerging Trends in Engineering and Applied Sciences (JETEAS), 5(7): 88-94.

[18] Versteg, H.K..; Malalasekera, W., 1995. An Introduction to Computational Fluid Dynamics: The Finite Volume Method. 1st ed. England: Longman, p.24.

[19] Menter, F.R.; Kuntz, M.; Langtry, R., 2003. Ten Years of Experience with the SST Turbulence Model. Turbulence, Heat and Mass Transfer, 4: 625-632.

[20] Nwaji, G.N.; Udongwo, S.; Ajayi, K.T.; Nwufo, O.C.; Onwuachu, C.C.; Ofong, I., 2021. Investigation of the Effect of Engine Speed on the Radial Inflow Turbine for Automotive Exhaust Energy Recovery, International Journal for research in Engineering & Technology, 1 (1): 1-15.

All © 2021 are reserved by International Journal of Advanced Science and Engineering. This Journal is licensed under a Creative Commons Attribution-Non Commercial-ShareAlike 3.0 Unported License.